JPET #87817

Pharmacoproteomic Effects

of Isoniazid, Ethambutol and SQ109 on

Mycobacterium tuberculosis H37Rv

Lee Jia, Lori Coward, Gregory S. Gorman, Patricia E. Noker, Joseph E. Tomaszewski

Developmental Therapeutics Program, National Cancer Institute, NIH, Rockville, Maryland (*L.J., J.E.T.*), Southern Research Institute, Birmingham, Alabama (*L.C., G.S.G., P.E.N.*)

Running title: Pharmacoproteomics of isoniazid, ethambutol and SQ109

Address correspondence to: Dr. Lee Jia, Rm 8042, 6130 Executive Blvd., National

Cancer Institute, NIH, Rockville, MD 20852. Telephone: 301-496-8777; Fax: 301-480-

4836; E-mail: jiale@mail.nih.gov

Number of text pages: 15

Number of tables: 2

Number of figures: 5

Number of references: 29

Number of words in Abstract: 247

Number of words in Introduction: 574

Number of words in Discussion: 1052

ABBREVIATIONS: MALDI-TOF, matrix-assisted laser desorption/ionization time-of-flight;

2-DE, two-dimensional polyacrylamide gel electrophoresis.

Recommended section: **Chemotherapy, Antibiotics, & Gene Therapy**

ABSTRACT

The present study was aimed at fingerprinting pharmacoproteomic alterations of the *Mycobacterium tuberculosis* H37Rv strain induced by antitubercular drugs isoniazid (INH), ethambutol (EMB), and SQ109 (a novel 1,2-diamine-based EMB analog), providing new understanding of pharmacoproteomic mechanisms of each and exploring new drug targets. The three drugs produced significant down-regulation of 13 proteins including immunogenic ModD, Mpt64, with proteins from the PE family being inhibited the most. Alternatively, the three drugs up-regulated 17 proteins including secreted antigenic proteins ESAT-6 and CFP-10. Among these, ESAT-6 and AphC were most effected by INH, while EMB had the greatest effect on ESAT-6. All three drugs produced only moderate up-regulation of aerobic and iron metabolism proteins, i.e., electron transfer flavoprotein Fix A and Fix B, and ferritin-like protein BfrB, suggesting that the interruption of microbacterial energy metabolism is not a primary mechanism of action. INH suppressed ATP-dependent DNA/RNA helicase, but up-regulated ß-ketoacyl-acyl carrier protein synthase. These effects may contribute to its bactericidal effects. In contrast, EMB and SQ109 did just the opposite: these drugs up-regulated the helicase and down-regulated the synthase. For most of the H37Rv proteins, similar pharmacoproteomic patterns were found for both EMB and SQ109. None of the drugs significantly regulated expression of chaperonins GroES, GroEL2 and Dnak, suggesting that these drugs do not affect chaperone-mediated nascent polypeptide folding and sorting. The present study identified proteins directly modulated by the actions of INH, EMB and SQ109, and distinguished INH activity from the diamine antitubercular compounds that inhibit *M. tuberculosis* H37Rv.

Introduction

The last decade witnessed a genomic gold rush that enriched our understanding of the genes, metabolism and intracellular processes of *Mycobacterium tuberculosis*, culminating in the recent publication of the complete genomic DNA sequence of the virulent strain H37Rv (Cole et al., 1998). Of the estimated 4000 encoded *M. tuberculosis* proteins, about 40% have known biochemical functions, another 44% have some sequence homology to known proteins in other bacterial systems, and 16% are completely unknown. Elucidation of the genomics and proteomics (Jungblut et al., 2001; Mattow et al., 2001) of the H37Rv strain offers valuable opportunities to explore drug targets and re-evaluate the mechanisms of action of well-established antitubercular drugs such as isoniazid (INH) and ethambutol (EMB) (American Thoracic Society, 2003) as an aid in developing new therapeutics, and to better define which functional genes are likely to be critical to survival and thus amenable as new drug targets. Selecting targets whose inactivation would lead to either bacterial death or stasis is not difficult; discovering how to exploit such targets and develop new active molecules in a time- and resource-efficient manner represents a more challenging enterprise.

Among this wealth of sequence information, emerging new techniques for monitoring differential gene expression offer valuable guidance in elucidating regulatory mechanisms of metabolic pathways and thereby pinpointing new drug targets. While DNA-based microarray is a well-developed new technology (Debouck and Goodfellow, 1999), proteomics can often provide more information than DNA-based expression arrays (Fields, 2001; Edwards et al., 2000). Proteomics not only provides the opportunity to determine the functional genome, but also facilitates the identification of proteins that have not been predicted by genome analysis. As an example, Jungblut et al. (2001) showed expression, by proteomic analysis, of six *M. tuberculosis* H37Rv genes that were not previously predicted by genomics. Analysis of the pharmacological effects of

drugs on the protein level is now called "Pharmacoproteomics" (Page et al., 1999), a discipline that studies interindividual variations in proteins in conjunction with pharmacological function and therapeutic response. These techniques can facilitate identification of new drug targets and provide information on mode of action of new or old drugs, which have traditionally remained unrecognized.

We have recently studied the *in vitro* and *in vivo* antitubercular effects of SQ109 (N-Geranyl-N'-(2-adamantyl)ethane-1,2-diamine; MW 330.2), a novel diamine developed from combinatorial chemistry and high-throughput screening around the [1,2]-diamine pharmacophore of EMB (Jia et al., 2005). SQ109 showed potency and efficacy in inhibiting intracellular *M. tuberculosis* that was less than INH, but superior to EMB. *In vivo* oral administration of SQ109 to the infected mouse model resulted in dose-dependent reductions of mycobacterial load in both spleen and lung comparable to that of EMB, but was less potent than INH (Jia et al., 2005). These study results, as well as decades of study records on EMB and INH, provide a conceptual framework for interpreting pharmacological effects of these drugs as cell-wall interrupters (Rozwarski et al., 1998; Mdluli et al., 1998; Wilson et al., 1999). Interestingly, systematic analysis and discovery of the precise gene products that are affected by these drugs using proteomic approaches have not yet been explored. To integrate existing genomic information with respective proteins and assess alterations induced by antitubercular drugs, we applied proteomic approaches based on two-dimensional polyacrylamide gel electrophoresis (2-D) combined with Matrix-Assisted Laser Desorption/Ionization-Time-Of-Flight (MALDI-TOF) and web-accessible microbial proteome databases (Pleibner et al., 2004) to investigate the dynamic pharmacoproteomic changes of *M. tuberculosis* H37Rv strains induced by the three drugs INH, EMB and SQ109.

Methods

Sample Preparation. Frozen stocks of *M. tuberculosis* H37Rv Pasteur were thawed and added to 400 ml of 7H9 broth medium supplemented with 0.2% glycerol, 10% albumin dextrose complex and 0.05% Tween 80, and incubated at 37^0C with shaking until the optical density (600 nm) of the medium reached 0.3. The culture was split into 5 separate flasks with different treatments: 1. EMB treatment at 1 MIC 24 µM (5 µg/ml); 2. INH treatment at 1 MIC 0.73 µM (0.1 µg/ml); 3. SQ109 treatment at 1 MIC 1.56 µM (628 ng/ml); 4. SQ109 treatment at 10 MIC 15.6 µM (6.28 µg/ml); and 5. untreated control. SQ109 dihydrochloride salt (MW 403.5) was used. To validate the drug-induced changes in protein structure, we conducted each treatment at the same time as the untreated control and under the same conditions. To elucidate the mechanisms by which the drugs inhibit bacteria, it was important to catalog where, when, and to what extent a specific drug affected the target protein. Therefore, we exposed the bacteria to the drugs at their MIC levels at the same time. For statistical analysis, five replicates of each treatment were prepared for individual 2-D and MALDI-TOF analyses. EMB and INH were prepared in distilled $H_2$0. SQ109 was prepared from 10 mM stock solution in methanol that was finally diluted with culture medium to the appropriate concentration for 1 and 10 MIC.

Each treated culture was incubated for 24 h at 37^0C with rolling. The bacteria were collected via centrifugation (3000 rpm, 4^0C for 10 min), and washed 3 times with PBS to remove BSA. The bacterial pellet was resuspended in 1.5 ml of lysis buffer composed of 9 M urea, 2% Triton X-100, 40 mM Tris freshly supplemented with phenylmethylsulfonyl fluoride (100 µg/ml) and leupeptin (2 µg/ml) in ultra pure distilled $H_2$0. Samples were homogenized six times in a Mini BeadBeater (Biospec, Inc. Bartlesville, OK) for 30s intervals at 4800 RPM with 0.1mm diameter glass beads. The lysates were removed from vials for proteomic analysis, and the protein concentrations

of each lysate were determined to be 2.80-3.08 mg/ml by Lowry protein assay (BioRad, Hercules, CA).

Two-dimensional Electrophoresis. Each of five replicate lysates from the above-mentioned five treatments was further diluted to 0.54 mg/ml of protein with a buffer composed of 9 M urea, 40 mM Tris, and 2% Triton X-100, 4% ampholytes and 10 µl/ml tributyl phosphine. The H37Rv protein was absorbed into IPG gel strips (pH 4-7, 11 cm) during overnight rehydration (13-15 h). 100 µg of protein was loaded onto each strip, and isoelectric focusing of the strips was carried out for 20 min at 250 volts, followed by a rapid ramp to 8000 volts for a total of 30,000 volt h. After focusing, the strips were equilibrated for 15 min with equilibration buffer 1 (75 mM tris, pH 8.8, 6 M urea, 2% SDS, 30% glycerol, 2% Dithiothreitol) followed by alkylation for 15 min using equilibration buffer 2 (75 mM tris, pH 8.8, 6 M urea, 2% SDS, 30% glycerol, 25 mg/ml iodoacetamide). SDS PAGE analysis of the equilibrated strips was performed in precast Criterion 8-16% gradient gels run for 60 min at 200 V using a Criterion dodeca cell. The gels were fixed for 60 min in 40% methanol and 10% acetic acid, and then stained overnight with Sypro Ruby Protein Gel Stain (BioRad, Hercules, CA). The gels were destained for 2 h with 10% methanol and 7% acetic acid to remove excess stain. Gel imaging was conducted using a Bio-Rad FX Pro Plus molecular imager interfaced to PDQuest software (version 7.1). Images were normalized by total gel density, and statistical analysis using the Mann-Whitney Signed-Rank test was performed on each of the treatment group (n= 5) pairs to demonstrate a 98% significance level between the groups. Regulation of the H37Rv proteins by the drugs was defined as a statistically significant change in intensities of protein spots compared to the matched untreated controls. Spots showing statistically significant regulation by the drugs were isolated and digested for protein identification.

MALDI-TOF Analysis of Tryptic Peptides. Proteins separated by 2-D were identified by MALDI-TOF analysis (Sloane et al., 2002). Tryptic digestion was carried out using a Montage trypsin digestion kit (Millipore Co., Bedford, MA). Briefly, protein spots of interest were excised and placed into individual wells of a ZipPlate. The samples were destained with a mixture of 25 mM ammonium acetate and 5% acetonitrile, followed by a mixture of 25 mM ammonium acetate and 50% acetonitrile. The solvent was removed under vacuum after each addition, and the gel pieces were dehydrated with acetonitrile. After removal of the acetonitrile, the proteins were digested overnight at $30^{o}C$ with sequencing grade modified porcine trypsin (Promaga, Madison, WI). Peptides were extracted from the gel by the addition of acetonitrile, followed by 0.2% trifluroacetic acid (TFA). Vacuum was applied to bind the peptides to the ZipPlate. The peptides were washed with 0.2% TFA and eluted with 15 ul of 0.1% TFA in 50% acetonitrile. The eluted peptides were mixed 1:1 or 1:5 with matrix (α-cyano-4-hydroxycinammic acid) dissolved in 0.1% TFA and 50% acetonitrile, spotted onto a gold plated MALDI target and analyzed on a Voyager Elite MALDI-TOF mass spectrometer (Perseptive, Framingham, MS). Measurements were performed in the reflection positive ion mode using the following parameters: 25 kV accelerating voltage, 74% grid voltage, 0.05% guide wire voltage, 100 ns delay and a low mass gate of 880 Da. Mass accuracy <100 ppm was obtained by internal calibration using trypsin autolysis peaks. Mass profiling for the known peptides was conducted on web-accessible microbial proteome databases (Pleibner et al., 2004) of the National Center for Biotechnology Information (NCBI) using the MASCOT Peptide Mass Fingerprint program with a mass tolerance of 100 ppm. A protein was regarded as identified if a Mascot search score was more than 51 (P< 0.05). If a protein did not receive a statistically significant Mascot score, its M_r and pI was compared to that of proteins identified in previously published maps (Mattow et al., 2001), and tentative identifications were assigned.

Results

Overall Proteomic Fingerprinting of *M. Tuberculosis* H37Rv.   Efficient separation of the H37Rv cellular proteins was achieved within the pI window of pH 4 to 7 and M_r window of 8 to 150 kDa. The Sypro Ruby stained 2-D patterns revealed about 575 distinct protein spots, varying by the amount of sample applied to the gels and the staining conditions. Among the 575 distinct spots seen on the gels, drug treatment significantly affected 44 of these spots, and we were able to structurally and functionally identify 20 of these in the present study. Table 1 summarizes these identified proteins, their M_r and pI values, known functions, and their corresponding accession numbers and open reading frame (ORF) Rv numbers from the NCBI protein database. The observed M_r and pI values of the proteins were calculated from their relative electrophoretic mobility. Proteins with a theoretical pI< pH 4 and a theoretical M_r <8 kDa were not identified probably because those highly acidic (pI< pH 4) and/ or very small (M_r < 6 kDa) proteins were not resolved by the 2-D technique (Molley, 2000; Gorg et al., 2004).

Among the identified proteins, production of the following proteins was moderately or significantly regulated by the tested drugs (Table 1): Spot 11 (ESAT-6, Rv3875) and 18 (CFP-10, Rv3874) which are secreted proteins that have been described as major T cell antigens of *M. tuberculosis*. These proteins stimulate interferon-gamma production in mouse and human T cells, and enhance macrophage activation and protect against mycobacterial infection (Wiker et al., 1999; Okkles et al., 2004). Spot 202 (AhpC, Rv2428) is a subunit of alkyl-hydroperoxide reductase, and may possess antioxidant activity that contributes to intracellular survival of the bacillus (Covert et al., 2001) and mediates toxic mechanisms of INH (Wilson et al., 1999). Spot 502 (ModD, Rv1860) is a major immunodominant antigen that has potential as a vaccine against tuberculosis (Cole et al., 1998; Mattow et al., 2001). Spot 1007 belongs to the PE multigene family whose genes are often based on multiple copies of the polymorphic

9

repetitive sequences referred to as PGRSs (Poulet and Cole, 1995). Spot 1201 (Mpt64, Rv1980c) was identified as an immunogenic protein (Fig. 1) found in unheated culture filtrates of *M. tuberculosis* H37Rv and in some strains of *M. bovis* (Yamaguchi et al., 1989). This antigen induces a strong delayed-type hypersensitivity reaction, and is used in studies on pathogenesis and cell-mediated immunology of *Mycobacteria*. Spots 1304 (Fix A, Rv3029c) and 1308 (Fix B, Rv3028c) are alpha- and beta-electron transfer flavoproteins serving as a specific electron acceptor for other dehydrogenases. They transfer electrons to the main respiratory chain via flavoprotein ubiquinone oxidoreductase (Cole et al., 1998), and participate in β-oxidation of fatty acids (Covert et al., 2001). Spot 2801 was identified as a complex of *acp*M (Rv2244) and *kas*A (Rv2245) gene products. The latter functions as a ketoacyl acyl carrier protein synthase for chain elongation of full length (~80 carbon) mycolic acids located in the cell wall (Cole et al., 1998). This protein forms the scaffold for attachment of mycosides and also catalyzes the condensation reaction of fatty acid synthesis by addition of two carbons from malonyl-ACP to acyl acceptor (Wilson et al., 1999). Spot 3103 (Bfrb, Rv3841) was identified a non-heme ferritin protein that is important in intracellular survival as the bacterial capacity to acquire iron in the vacuole is limited. Spot 6302 was identified as ATP-dependent DNA/RNA helicase (Rv3649) (Cole et al., 1998).

Among the identified proteins, the following were not significantly regulated by the tested drugs probably, due to their lack of signal sequences and /or ability to elicit IFN-gamma (Wiker et al., 1999): Spot 1003 was annotated as a molecular chaperonin-10 (GroES, Rv3418c) that behaves as a co-chaperonin to cap the ends of GroEL (the bacterial homolog of Hsp60). Spots 2706 (Dnak, Rv0351) acts as a chaperonin and spot 3702 (GroEL2, Rv0440) belongs to a class know as heat shock proteins. Chaperones are located in every cellular compartment, bind a wide range of proteins, and may be part of a general protein-folding mechanism. In bacteria, ~85% of the proteins are

released from their chaperones and go on to fold and sort normally. Chaperones are required for folding and unfolding of proteins and the assembly of multimeric protein complexes (Cole et al., 1998). No significant pharmacoproteomic effects on the chaperones were found, suggesting that these drugs do not affect chaperone-mediated nascent polypeptide folding, sorting and conformational modification. Since its expression was not changed by drug exposure, the abundance of spot 1003 was used as an internal control for drug-treated and untreated H37Rv samples for validation purpose in the present study.

Pharmacoproteomic Effects of INH, EMB and SQ109 on *M. tuberculosis* H37Rv. Generally, treatment of the H37Rv with INH, EMB and SQ109 resulted in changes of about 44 protein spots, although the biological function and identity of some of these proteins are still unknown and may ultimately account for specific antimycobacterial drug action (Table 2). Thirty of these spots were further analyzed by MALDI-TOF, and among them 20 were identified (Table 1). Some of the identified proteins that were regulated by the tested drugs are shown in Table 2. INH, EMB and/ or SQ109 significantly down-regulated the following spots (P< 0.05, Mann-Whitney Signed-Rank test): 109, 501, 502 (ModD, Rv 1860), 1007 (PE protein), 1201 (Mpt64), 1301 (Trps), 1408, 3304, 4001, 4003, 5001 (Esx), 7202, and 8606. Whereas, INH, EMB and/ or SQ109 up-regulated spots 11 (ESAT-6), 16, 18 (CFP-10), 102, 103, 106, 201, 202 (AhpC), 302, 1208 (Rv0207), 5104, 7002 (Rv3865), 8109 (LppD), 8112, and 8207. Figure 2 demonstrates the up- and down-regulation of proteins ESAT-6, CFP-10, PE and others. In general, these drugs remarkably suppressed immunological proteins (T cell antigens) such as ModD, Mpt64 and the PE family. The inhibition may produce the drugs' pharmacological effects on pathogenesis and cell-mediated immunology, and therefore, reduce H37Rv-induced hypersensitivity reaction. The drugs up-regulated ESAT-6 family proteins including CFP-10 (Fig 2), and a subunit of the alkyl-

hydroperoxide reductase, AhpC (Rv2428). A previous report that transcripts for AhpC are induced by INH (Wilson et al., 1999) is consistent with the results reported here, and it helps further validate the findings of present pharmacoproteomic analysis.

Treatment of H37Rv with INH, EMB and SQ109 produced moderate increases in gene expression (12~35%) of two-component subunits of electron transfer flavoprotein Fix A (Rv3029, i.e., spot 1304) and Fix B (Rv3028, i.e., spot 1308), and the ferrtin-like proteins encoded by *bfrB* (Rv3841, i.e., spot 3103) (Table 2). This suggests that it is unlikely that these three drugs inhibit the bacteria by primarily interrupting aerobic and iron metabolism of *M. tuberculosis*, although the aerobic metabolism genes (Sherman et al., 2001) and iron metabolism genes (Rodriguez et al., 2002) become important in intracellular survival as mycobacterium faces a microaerophilic and nutrient-limited environment within the host and its capacity to acquire enough oxygen and iron is limited.

Of particular interest in these studies, INH alone up-regulated spot 2801, identified as a complex of acpM and kasA (β-ketoacyl-acyl carrier protein synthase), in contrast, EMB and its 1,2-diamine analog SQ109 inhibited the complex expression (Fig. 3, 4; Table 2). As presented in Fig. 4, the complex was clearly identified on the basis of 5 matching peptides. The up-regulation of the complex at the proteomic level by INH was coincidently in line with Wilson's findings (Wiker et al., 1999) from microarray hybridization that INH induced *kasA* gene that encodes the protein physiologically relevant to the mode of INH action. Another difference in pharmacoproteomic effects on H37Rv between INH and the 1,2-diamine analogs is that bactericidal INH suppressed ATP-dependent DNA/RNA helicase, by contrast, EMB and SQ109 up-regulated the two gene products. The opposite regulation by the two classes of anti-tuberculosis drugs may reflect their differences in *in vitro* antituberculosis effect reported by us (Jia et al., 2005), showing that INH inhibits H37Rv growth more potently than SQ109 and EMB.

Although there were slight differences in regulatory potency between EMB and SQ109, the two drugs exhibited similar pharmacoproteomic effects on the H37Rv probably due to their shared 1,2-diamine pharmacophore.

Our previous study (Jia et al., 2005) demonstrated that SQ109 at 0.5, 1, 2 and 4 MIC levels exhibited in vitro antimicrobial activity against M. tuberculosis H37Rv grown inside the host murine macrophage cells in a dose-dependent fashion. This inhibition may be a collective consequence of SQ109 elicited both down-regulation of the following protein spots 501, 502 (ModD), 1007 (PE), 1201, 1301 (TrpS), 3304, 5001, and up-regulation of the following spots: 11 (ESAT-6), 18 (CFP-10), 102, 103, 106, 202 (AhpC), 302, 1208 (Rv0207), 1304 (Fix A), 7002 (Rv3865), 8109 (LppD), 8112, and 8207 because the SQ109-induced regulation also exhibited dose-dependency (Table 2) although the precise implications of pharmacoproteomic action of SQ109 to its integrated antitubercular effects need further investigation. Figure 5 showed some of the identified proteins that were regulated by SQ109 dose-dependently.

Discussion

In searching for novel protein targets for drug intervention, we initiated the systemic pharmacoproteomic investigation of the effects of first-line antituberculosis drugs INH and EMB on protein composition of H37Rv with those of the new investigational drug SQ109. We reproducibly detected distinct changes in H37Rv cellular proteins following individual drug treatments. The present comparative pharmacoproteomic analysis revealed that all three drugs specifically targeted the ESAT-6 family, including CFP10, resulting in up-regulation of the protein expression with the potency order EMB> INH> SQ109. ESAT-6 was first identified in 1995 (Wiker et al., 1999) as a well-known early secreted antigenic target, which is essential for virulence of *M. tuberculosis* (Hsu et al., 2003). ESAT-6 is involved in cell wall and cell processes (Marques et al., 2004), and appears as eight triplet spots divided into two groups, each group consisting of four spots, including two full length of ESAT-6. Post-translational modification of ESAT-6 has recently been reported (Okkels et al., 2004). CFP-10 is a 10 kDa culture filtrate protein and member of the ESAT-6 family with secretary antigenic function. The up-regulation of the proteins by the drugs may have pharmacological significance of induction of protective immune responses against *M. tuberculosis* challenge because the proteins are dominant T-cell determinant in *M. tuberculosis* infection of human and animals (Andersen et al., 1995). The concept is further enforced by a recent report that recombinant *M. bovis* Bacillus Calmette-Guērin (BCG) secreting ESAT-6 confers enhanced protection against tuberculosis in mice compared to wide-type BCG (Pym et al., 2003).

Up-regulation of β-ketoacyl-acyl carrier protein synthase synthesis was detected after INH treatment for 20 or 30 min at 1 mg/ml by Wilson et al (1999), and Mdluli et al (1998). The similar induction of the complex of acpM and kasA was also found in the present study (Fig. 3, 4) at a lower INH level (0.1 mg/ml) after longer exposure (24 h).

The related results are consistent and indicate that interruption of the type II fatty acid synthase (FAS-II) cycle is rapidly sensed and responded to at a transcriptional level within a fraction of a generation time (24-36 h) of *M. tuberculosis.* INH blocks the mycolic acid biosynthesis of cell-wall lipids and genes responsible for lipid metabolism after its activation by the mycobacterial catalase-peroxidase enzyme KatG. Although the precise mechanism of INH-mediated killing remains unresolved, INH is believed to target three FAS-II complex proteins by binding to NADH in the pocket of enoyl-acyl carrier protein (ACP) reductase, InhA (Rozwarski et al., 1998). INH may also form a covalent trimolecular complex with KasA and AcpM (an acyl carrier protein) (Mdluli et al., 1998) designated as spot 2801 in the present study, and thus block the mycolic acid biosynthetic pathway at the transcriptional level which would be reflected by parallel changes in the abundance of the corresponding transcripts (Wilson et al., 1999). As a consequence of INH activity, mature mycolates are not produced and become progressively depleted. At the same time, an intracellular accumulation of saturated fatty acids (C24-C26) occurs and implies that the induction of KasA and AcpM genes is the consequence of a regulatory feedback mechanism that senses the imbalance of mycolic acid biosynthetic intermediates (Mdluli et al., 1998). Specific up-regulation of the complex by INH represents an important potential target for future development of INH-like therapeutics but not for the EMB-like mode because the two 1,2-diamine analogs regulated the complex differently from INH (Fig. 3).

AhpC is a subunit of the alkyl-hydroperoxide reductase that detoxifies cells by reducing specific classes of reactive oxygen species (Wilson et al., 1999). It is likely that this gene product contributes to drug-resistant tuberculosis strains. In view of the degree of up-regulation by 2.66 and 2.12 folds of AhpC (Table 2) expression by INH and EMB, which are well-known drugs to produce resistant strains, while SQ109 at the same MIC level showed the potency similar to the two in regulating the AhpC, it would be of interest

to investigate whether SQ109 has probability of inducing resistant strains. The study may further clarify the involvement of AhpC in development of drug resistance.

All three drugs significantly suppressed PE protein spot 1007 (Fig. 2, Table 2). The name of PE derives from the motifs Pro-Glu (PE) found near the N terminus of the acidic, glycine-rich proteins. The 99 members of the PE protein family all have a highly conserved N-terminal domain of ~110 amino acid residues that is predicted to have a globular structure, followed by a C-terminal segment that varies in size, sequence and repeat copy number. It has been proposed that 1) the PE protein could represent the principal source of antigenic variation in what is otherwise a genetically and antigenically homogeneous bacterium; and 2) the glycine-rich protein might interfere with immune response by inhibiting antigen processing (Cole et al., 1998). Although the subcellular location of the PE is unknown, and it is too early to attribute biological functions to the PE family, it is tempting to hypothesize that, based on the present finding that all three drugs showed the most potent inhibition on the PE (Table 2), PE could be a common target of at least, the two classes of anti-tuberculosis drugs INH and EMB, and it may be used as an efficacy biomarker to indicate tuberculosis inhibition, and pharmacologic responses to antituberculosis therapeutics.

Despite overall similarity of the proteomic patterns between Mattow's report (2001) and the present study, differences in spot amount and intensity were observed between Mattow's sliver stain techniques and our Sypro Ruby stain. The differences are probably due to the variable response of the proteins to the staining procedures and conditions although Sypro Rudy stain has been considered very compatible with in-gel digests for mass spectrometry and has a linear dynamic range of 2-2000 ng, spanning the ranges of both Coomassie and sliver stains (Lopez, 2000).

Proteomics-based molecular interaction screening approaches are generally more suitable for the identification of direct drug targets (Kley et al., 2004). Mass

16

spectrometry analysis following 2D in a typical proteomics workflow is a key step that

helps determine various characteristics about the proteins in question. These

pharmacoproteomic alterations explain the mechanisms of actions of individual drugs,

and may pinpoint the apoptotic targets of each drug. Knowledge of the putative

pharmacoproteomic mechanisms will promote better use of existing drugs and facilitate

the conception of new therapies and new drug development.

JPET #87817

References

AMERICAN THORACIC SOCIETY DOCUMENTS (2003) American Thoracic Society/Centers for Disease Control and Prevention/ Infectious Diseases Society of America: Treatment of Tuberculosis. *Am J Respir Crit Care Med* **167:**603-662.

Andersen P, Andersen AB, Sorensen AL and Nagai S (1995) Recall of long-lived immunity to *Mycobacterium tuberculosis* infection in mice. *J Immunol* **154:**3359-3372.

Cole ST, Brosch R, Parkhill J, Garnier T, Churcher C, Harris D, Gordon SV, Eiglmeier K, Gas S, Barry III CE, Tekaia F, Badcock K, Basham D, Brown D, Chillingworth T, Connor R, Davies R, Devlin K, Feltwell T, Gentles S, Hamlin N, Holroyd S, Hornsby T, Jagels K, Krogh A, McLean J, Moule S, Murphy L, Oliver K, Osborne J, Quail MA, Rajandream MA, Rogers J, Rutter S, Seeger K, Skelton J, Squares R, Squares S, Sulston JE, Taylor K, Whitehead S, and Barrell BG (1998) Deciphering the biology of Mycobacterium tuberculosis from the complete g enome sequence. [published erratum appears in Nature **396:**190, 1998] *Nature* **393:** 537-544.

Covert BA, Spencer JS, Orme IM and Belisle JT (2001) The application of proteomics in defining the T cell antigens of Mycobacterium tuberculosis. *Proteomics* **1:**574-586.

Debouck C and Goodfellow PN (1999) DNA microarrays in drug discovery and development. *Nat Genet* **21**(Suppl 1): 48-50.

Edwards AM, Arrowsmith CH and Pallieres BD (2000) Proteomics: new tools for a new era. *Modern drug discovery* **3:** 34-44.

Fields S. (2001) Proteomics in genomeland. *Science* **291:**1221-1224.

Gorg A, Weiss W and Dunn M. (2004) Current two-dimensional electrophoresis technology for proteomics *Proteomics* **4:**3665-3685.

Hsu T, Hingley-Wilson SM, Chen B, Chen M, Dai AZ, Morin PM, Marks CB, Padiyar J, Goulding C, Gingery M, Eisenberg D, Russell RG, Derrick SC, Collins FM, Morris SL, King CH, and Jacobs Jr. WR (2003) The primary mechanism of attenuation of bacillus Calmette–Guérin is a loss of secreted lytic function required for invasion of lung interstitial tissue. *Proc Natl Acad Sci USA* **100:**2420-12425.

Jia L, Tomaszewski EJ, Hanrahan C, Coward L, Noker EP, Gorman SG, Nikonenko B and Protopopova M (2005) Pharmacodynamics and pharmacokinetics of SQ109, a new diamine-based antitubercular drug. *Br J Pharmacol* **144:** 80-87.

Jungblut PR, Muller EC, Mattow J and Kaufmann SHE (2001) Proteomics reveals open reading frames in Mycobacterium tuberculosis H37Rv not predicted by genomics. *Infect Immu* **69**: 5905-5907.

Kley N, Ivanov I and Meier-Ewert S (2004) Genomics and proteomics tools for compound mode-of-action studies in drug discovery. *Pharmacogenomics* **5:**395-404.

Lopez MF (2000) Better approaches to finding the needle in a haystack: Optimizing proteome analysis through automation. *Electrophoresis* **21**:1082-1093.

Marques MA, Espinosa BJ, Xavier da Silveira EK, Pessolani MCV, Chapeaurouge A, Perales J, Dobos K, Belisle J, Spencer JS and Brennan PJ (2004) Continued proteomic analysis of Mycobacterium leprae subcellular fractions *Proteomics* **4:** 2942-2953.

Mattow J, Jungblut PR, Muller EC and Kaufmann SHE (2001) Identification of acidic, low molecular mass proteins of Mycobacterium tuberculosis strain H37Rv by matrix-

assisted laser desorption/ionization and electrospray ionization mass spectrometry. *Proteomics* **1:** 494-507.

Mdluli K, Slayden RA, Zhu Y, Ramaswamy S, Pan X, Mead D, Crane DD, Musser JM and Barry III CE. Inhibition of a Mycobacterium tuberculosis β-Ketoacyl ACP Synthase by Isoniazid. *Science* **280:** 1607-1610.

Molloy M. (2000) Two-dimensional electrophoresis of membrane proteins using immobilized pH gradients. *Anal Biochem* **280:**1-10.

Okkels LM, Müller E, Schmid M, Rosenkrands I, Kaufmann SHE, Andersen P and Jungblut PR (2004) Current two-dimensional electrophoresis technology for proteomics *Proteomics* **4:** 2954-2960.

Page MJ, Amess B, Rohlff C, Stubberfield C and Parekh R. (1999) Proteomics: a major new technology for the drug discovery process. *DDT* **4:**55-62

Pleibner K, Eifert T, Buettner S, Schmidt F, Boehme M, Meyer TF, Kaufmann SHE and Jungblut PR. (2004) Web-accessible proteome databases for microbial research. *Proteomics* **4**:1305-1313.

Poulet S and Cole ST (1995) Characterization of the polymorphic GC-rich repetitive sequence (PGRS) present in Mycobacterium tuberculosis. *Arch Microbiol* **163:** 87-95.

Pym AS, Brodin P, Majlessi L, Brosch R, Demangel C and Cole ST (2003) Recombinant BCG exporting ESAT-6 confers enhanced protection against tuberculosis. *Nat Med* **9:** 533-539.

Rodriguez GM, Voskuil MI, Gold B, Schoolnik GK, Smith I (2002) An essential gene in Mycobacterium tuberculosis: Role of IdeR in iron-dependent gene expression, iron metabolism, and oxidative stress response. *Infect Immun* **70:** 3371-3381.

Rozwarski DA, Grant GA, Barton DHR, Jacobs Jr. WR and Sacchettini JC. (1998) Modification of the NADH of the Isoniazid Target (InhA) from *Mycobacterium tuberculosis Science* **279:** 98-102.

Sherman DR, Voskuil M, Schnappinger D, Liao R, Harrell MI and Schoolnik GK. (2001) Regulation of the Mycobacterium tuberculosis hypoxic response gene encoding alpha-crystallin. *Proc Natl Acad Sci USA* **98:** 7534-7539.

Sloane AJ, Duff JL, Wilson NL, Gandhi PS, Hill CJ, Hopwood FG, Smith PE, Thomas ML, Cole RA, Packer NH, Breen EJ, Cooley PW, Wallace DB, Williams KL and Gooley AA. (2002) High throughput peptide mass fingerprinting and protein macroarray analysis using chemical printing strategies. *Mol Cell Proteomics* **1:**490-499.

Wilson M, DeRisi J, Kristensen H, Imboden P, Rane S, Brown P and Schoolnik G. (1999) Exploring drug-induced alterations in gene expression in Mycobacterium tuberculosis by microarray hybridization. *Proc Natl Acad Sci USA* **96**:12833-12838.

Wiker HG, Michell SL, Hewinson RG, Spierings E, Nagai S and Harbose M (1999) Cloning, expression and significance of MPT53 for identification of secreted proteins of mycobacterium tuberculosis. *Microb Pathog* **26:** 207-219.

Yamaguchi R, Matsuo K, Yamazaki A, Abe C, Nagai S, Terasaka K and Yamada T (1989) Cloning and characterization of the gene for immunogenic protein MPB64 of Mycobacterium bovis BCG. *Infect Immun* **57**: 283–288.

Footnotes

The studies described here were part of the National Cancer Institute, National Institute of Allergy and Infectious Diseases project approved by the Inter-institute Program of National Institutes of Health, and supported by National Cancer Institute funds N01-CM-07110 and N01-CM-52203.

Legends for Figures

Fig. 1. MALDI-MS spectra from spot 1201, down-regulated by all the three drugs, was identified as Mpt64 (Rv1980c) protein from a Mascot search. Ions and their sequence corresponding to the theoretical tryptic digest peptide masses of the protein are m/z 1136.6 (FLSAATSSTPR), 1170.5 (AFDWDQAYR), 1193.6 (SLENYIAQTR), 1379.7 (DKFLSAATSSTPR), 1636.8 (VYQNAGGTHPTTTYK), and 2220.1 (EAPYELNITSATYQSAIPPR).

Fig. 2. Comparison of 2-D images of cellular proteins of *M. Tuberculosis* H37Rv treated with INH, EMB and SQ109 at their MICs, respectively. A, untreated control; B, INH treatment; C, EMB treatment; D, 10-fold MIC of SQ109 treatment. Note quantitative and qualitative changes in protein expression following the treatments: INH, EMB and SQ109 significantly up-regulated spots 11 (ESAT-6), and 18 (CFP-10), while down-regulated spots 1007 (PE protein), and 4003.

Fig. 3. Differences between regulation of spot 2801, identified as a complex of AcpM and KasA proteins, by INH and the two 1,2-diamine analogs EMB and SQ109. Note INH alone up-regulated the complex. To the contrary, EMB and SQ109 down-regulated the complex expression.

Fig. 4. MALDI-MS spectra from spot 2801, identified as a complex of AcpM and KasA from a Mascot search (Matrix Science) of the tryptic peptides. Peptides matched AcpM were 1097.5 (IPDEDLAGLR), 1468.7 (LEEENPEAAQALR), 1611.7 (IESEVPDAVANVQAR, and 1810.9 (AKIESENPDAVANVQAR). Peptides matched to KasA were 1090.5 (ASRPFDKDR), and 1331.7 (FAVVVGTGLGGAER).

Fig. 5. SQ109-induced pharmacoproteomic changes of the known proteins of H37Rv in

a concentration-dependent manner. The results are presented as % change (means ±

SE, n=5) of SQ109-induced protein expression based on the untreated control.

Table 1. Identity of *M. tuberculosis* H37Rv proteins*.

Spot #	Name and Rv #	NCBI #	Protein function	Observed Mr (kDa)	Predicted Mr (kDa)	Observed pI	Predicted pI	Mascot score
11	ESAT-6 (Rv3875)	2960227	Early secreted antigenic target-6; essential for virulence; may elicit IFN-γ from memory effector cells	9.0	9.8	4.4	4.48	16
18	CFP-10 (Rv3874)	15611010	Secreted antigenic CFP-10 antigen, belongs to the ESAT-6 (esx) family	10.5	10.8	4.6	4.59	98
202	AhpC (Rv2428)	15609565	Alkyl hydroperoxide reductase	21.8	21.7	4.5	4.50	60
502	ModD (Rv1860)	15608997	Major immunodominant antigen	47.9	32.7	4.4	4.93	47
1003	GroES (Rv3418c)	15825763	Chaperonin-10	9.8	10.7	4.7	4.6	114
1007	Probable PE	15608335	Immunogenic importance	9.5	9.6	4.8	4.56	26
1201	Mpt64 (Rv1980c)	15609117	Immunogenic protein	22.1	24.8	4.6	4.84	101
1208	Rv0207c	15607348	Hypothetical protein	26.9	26.2	4.8	4.72	64
1301	TrpS (Rv3336c)	15610472		29.2	36.4	4.6	5.1	40
1304	Fix A (Rv3029c)	15610165	alpha-electron transfer flavoprotein	30.7	31.7	4.7	4.7	76
1308	Fix B (Rv3028c)	15610165	β-electron transfer flavoprotein	28.5	31.7	4.8	4.7	63
2706	Dnak (Rv0350)	15607491	70 KDa heat shock protein	60.1	66.8	4.9	4.85	145
2801	acpM(Rv2244)	15609381	Acyl carrier protein	65.7	12.5	4.8	3.9	67
	KasA (Rv2245)	15609382	β-ketoacyl synthase		43.3		5.1	30
3103	BfrB (Rv3841)	15610977	Non-heme ferritin family protein	18.3	20.4	5.0	4.7	78
3702	GroEL2 (Rv0440)	15607581	Chaperonin-2 heat-shock protein	55.6	56.7	5.1	4.85	207
5001	Rv1038c	15608178	The ESAT-6 (esx) family	10.4	11.0	5.4	5.2	40
6302	Rv3649	15610785	ATP-dependent DNA/RNA helicase	29.5	81.9	5.7	5.8	30
7002	Rv3865	15611001	Hypothetical protein	9.0	10.6	6.0	6.0	43
8109	LppD (Rv1899c)	15609036	Lipoprotein	16.9	35.5	6.7	10.2	63

*A protein was regarded as identified if the matched peptides covered at least

30% of the complete protein sequence. Tentative identifications were given

to proteins with Mascot scores< 51.

Table 2. Individual proteographic changes of gel intensity in ratios based on the non-treatment control. The H37Rv was treated with the drugs at their MICs, or 10-fold MIC (10x).

Spot#	Name	M_r	pI	EMB	INH	SQ109	SQ109 (10x)
3		9.2	4.3	1.55*	1.16	0.90	0.94
6		12.5	4.3	1.20	1.23	1.11	0.92
11	ESAT-6	9.0	4.4	3.31*	2.29*	1.28	2.10*
16		11.7	4.5	1.26	1.64*	1.29	1.10
18	CFP-10	10.5	4.6	2.11*	1.86*	1.08	1.82*
102		19.9	4.3	1.52	1.51	1.25	1.72*
103		19.7	4.3	1.21	1.22	1.39	1.65*
106		14.0	4.4	1.13	1.38	1.19	1.62*
109		13.5	4.5	0.66	0.77	0.82	0.58*
111		17.9	4.6	1.06	1.11	1.15	1.39
201		23.5	4.4	1.03	1.55	1.34	1.59*
202	AhpC	21.8	4.5	2.12*	2.66*	1.96*	4.00*
302		31.2	4.4	1.28	1.71*	1.48	1.61*
501		42.3	4.4	0.37*	0.02*	0.87	0.03*
502	ModD	47.9	4.4	0.80	0.26*	0.55*	0.37*
1001		12.7	4.6	1.11	0.99	1.34	0.88

1003	GroES	9.8	4.7	0.96	0.81	0.84	0.96
1007	PE	9.5	4.8	0.03*	0.02*	0.78*	0.36*
1201	Mpt64	22.1	4.6	0.44*	0.27*	0.78	0.65*
1208	Rv0207c	26.9	4.8	1.16	1.42	1.23	2.27*
1301	TrpS	29.2	4.6	0.45*	0.28*	1.00	0.41*
1304	Fix A	30.7	4.7	1.18	1.30	1.12	1.35
1308	Fix B	28.5	4.8	1.07	1.03	0.68	1.44
1408		35.5	4.7	0.78	0.87	0.79	0.68*
2103		19.0	4.8	1.28	1.24	1.12	1.19
2108		14.1	4.9	1.11	1.27	0.96	1.20
2706	Dnak	60.1	5.9	0.76	0.88	0.77	0.81
2801	AcpM/KasA	65.7	4.8	0.85	1.97*	0.62*	0.73
3103	BfrB	18.3	5.0	1.05	1.58	1.14	0.71
3201		22.1	5.0	1.14	1.15	0.82	0.70
3304		28.0	5.0	0.51*	0.22*	0.59*	0.22*
3702	GroEL2	55.6	5.1	0.79	1.09	1.12	1.05
4001		13.0	5.2	0.57*	0.85	0.40*	0.89
4003		10.1	5.3	0.02*	0.01*	0.69*	0.02*
4410		35.8	5.4	1.21	1.07	0.85	1.75
5001	ESAT-6(esx)	10.4	5.4	0.92	0.52*	0.87	0.50*
5104		16.1	5.6	1.23	1.33	1.49	1.42
5106		16.8	5.6	0.91	0.66	0.95	1.19
5408		40.9	5.6	0.89	0.94	0.72	1.24

6302	Helicase	29.5	5.7	1.22	0.57*	1.29	1.42
7002	Rv3865	9.0	6.0	1.36	1.30	1.36	1.88*
7202		23.3	5.9	0.74*	0.89	0.62*	0.41*
8002		9.9	6.3	0.94	0.96	0.76	1.32
8109	LppD	16.9	6.7	1.51*	1.97*	1.37	2.17*
8112		17.3	6.9	1.02	1.60*	1.01	1.52*
8207		23.8	6.8	1.31	1.64*	1.22	1.30
8606		49.2	6.9	0.86	0.78	0.51*	0.52*

_____

* indicates a significant change from either the control group or between

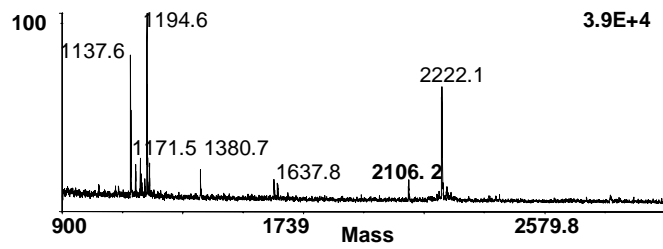treatment groups (Mann-Whitney Signed-Rank test, 98% significance), n=5 per
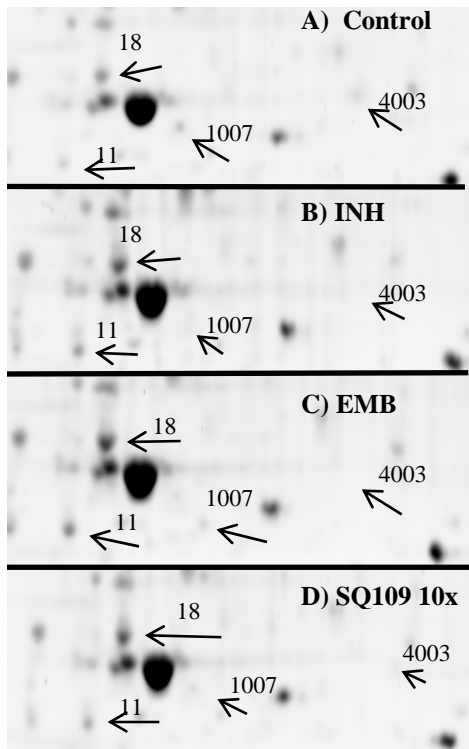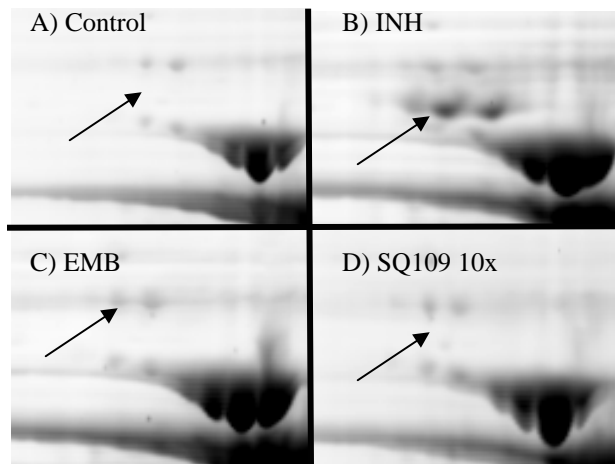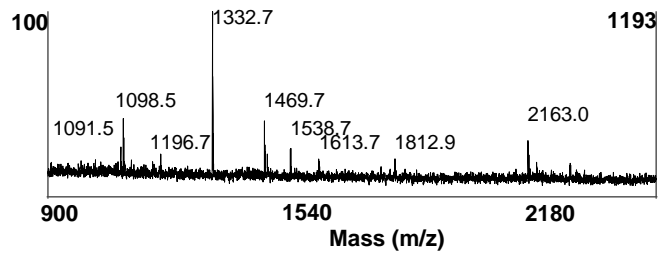
group.

Fig. 1

Fig. 2.

Fig. 3

A) Control   B) INH

C) EMB   D) SQ109 10x

Fig. 4

Fig. 5